



LAWRENCE
LIVERMORE
NATIONAL
LABORATORY

High precision measurements of the diamond Hugoniot in and above the melt region

D. Hicks, T. Boehly, P. Celliers, D. Bradley, J. Eggert, R. S. McWilliams, G. Collins

August 11, 2008

Physical Review B

Disclaimer

This document was prepared as an account of work sponsored by an agency of the United States government. Neither the United States government nor Lawrence Livermore National Security, LLC, nor any of their employees makes any warranty, expressed or implied, or assumes any legal liability or responsibility for the accuracy, completeness, or usefulness of any information, apparatus, product, or process disclosed, or represents that its use would not infringe privately owned rights. Reference herein to any specific commercial product, process, or service by trade name, trademark, manufacturer, or otherwise does not necessarily constitute or imply its endorsement, recommendation, or favoring by the United States government or Lawrence Livermore National Security, LLC. The views and opinions of authors expressed herein do not necessarily state or reflect those of the United States government or Lawrence Livermore National Security, LLC, and shall not be used for advertising or product endorsement purposes.

High precision measurements of the diamond Hugoniot in and above the melt region

D. G. Hicks,^{1,*} T. R. Boehly,² P. M. Celliers,¹ D. K. Bradley,¹ J. H. Eggert,¹ R. S. McWilliams,^{1,3} and G. W. Collins¹

¹*Lawrence Livermore National Laboratory, Livermore, CA 94550*

²*Laboratory for Laser Energetics, University of Rochester, NY 14623*

³*University of California, Berkeley, CA*

(Dated: August 1, 2008)

High precision laser-driven shock wave measurements of the diamond principal Hugoniot have been made at pressures between 6 and 19 Mbar. Shock velocities were determined with 0.3-1.1% precision using a velocity interferometer. Impedance matching analysis, incorporating systematic errors in the equation-of-state of the quartz standard, was used to determine the Hugoniot with 1.2-2.7% precision in density. The results are in good agreement with published *ab initio* calculations which predict a small negative melt slope along the Hugoniot, but disagree with previous laser-driven shock wave experiments which had observed a large density increase in the melt region. In the extensive solid-liquid coexistence regime between 6 and 10 Mbar these measurements indicate that the mixed phase may be slightly more dense than would be expected from a simple interpolation between liquid and solid Hugoniots.

PACS numbers: 52.50.Lp, 62.50.+p, 64.70.Dv, 71.30.+h

I. INTRODUCTION

Carbon has the highest melting temperature of any element at ambient conditions (~ 4000 K), a manifestation of its unusually large cohesive energy.^{1,2} The diamond phase, with its open yet compact structure, is stable up to extremely high pressures and remains the only observed high pressure phase of carbon. Such compactness and stability is attributable to the absence of core p electrons which allows valence p electrons closer to the nucleus and creates remarkably strong sp^3 bonds.³ The study of diamond melting at high pressures thus provides a valuable window into the limiting behavior of strongly-bonded materials.

After early predictions by Bundy⁴ had suggested that the melt line of diamond, in analogy with that of Si and Ge, had a negative slope, experiments by Shaner *et al.*⁵ along with numerous models⁶⁻⁸ indicated instead that the melt line was positive. With an improved understanding of the structure of liquid carbon, predictions showed that diamond, like graphite, had a maximum in the melt line near 5 Mbar.⁹⁻¹² The diamond phase was calculated to be stable up to around 11 Mbar, above which the BC8 phase was favored^{9,12,13} although this new phase has yet to be observed.

Shock wave experiments are currently the only method by which the diamond melt can be studied experimentally. Shocked graphite explores the positive slope region of the diamond melt line,^{5,14} while shocked diamond, with its higher starting density, probes the negative slope region. Calculations of the diamond Hugoniot were recently made using density-functional based molecular dynamics calculations. Correa *et al.*^{9,15} indicate that melting along the diamond Hugoniot extends over an unusually large solid-liquid coexistence regime between 6 and 10 Mbar, crossing the diamond-BC8-liquid triple point at 9 Mbar. Romero and Mattson¹⁶ predicted a similar Hugoniot although they did not independently calculate

the melt line, depending instead on the phase boundaries given by Wang *et al.*¹⁰ and Correa *et al.*⁹ Optical reflectivity measurements by Bradley *et al.*¹⁷ showed that shocked diamond transforms into a conducting fluid between 6 and 10 Mbar, the region of the predicted solid-liquid coexistence region.

Measurements of the diamond Hugoniot in its solid phase were performed by Pavlovskii¹⁸ and Kondo and Ahrens.¹⁹ Much higher pressures were studied by Nagao *et al.*²⁰ and Brygoo *et al.*²¹ using laser-driven shocks. Brygoo *et al.* observed a dramatic increase in density at around 7.5 Mbar which they concluded was caused by melting. This distinct feature was not found in *ab initio* calculations^{15,16} raising the interesting possibility of whether the slope of the diamond melt line is significantly more negative than predicted. Ultimately, however, most of the laser-driven shock wave measurements of Nagao *et al.*²⁰ and Brygoo *et al.*²¹ had significant error bars and do not tightly constrain the equation-of-state of carbon near the diamond melt line.

In this paper, improved measurements of the diamond Hugoniot in and above the melt region are described. Shock waves driven by a high-power laser were delivered to a diamond target via a quartz pusher. High precision measurements of shock velocities were made using a time-resolved velocity interferometer. Impedance matching calculations with quartz as the reference standard were then used to determine the pressure, density, and particle velocity in diamond. The results are generally in agreement with *ab initio* predictions and do not show a large density increase at melting. In Section II details of the experimental apparatus are described; Section III describes the improvements which allowed particularly high precision velocity measurements to be made; Section IV outlines the impedance matching calculations; Section V shows the results, describing the random and systematic errors which were quantified and other systematic errors which were discounted; Section VI compares these results

with previous measurements and theories.

II. EXPERIMENT

The experiment was performed on the OMEGA laser facility at the University of Rochester, a neodymium-doped phosphate glass system operating with frequency-tripled, $0.35\ \mu\text{m}$ light.²² To generate the shock pressures explored in these experiments, laser energies between 300 and 1000 J were delivered using a temporally square pulse of either 2 or 3 ns in duration. The laser focal spot was smoothed using distributed phase plates producing near uniformly-irradiated spots of either 600 or 800 μm in diameter, depending on the experiment. This resulted in average laser intensities between 3 and $9 \times 10^{13}\ \text{W}/\text{cm}^2$.

Targets consisted of 500 μm thick type Ia or IIa diamond oriented along the (110) axis and glued onto either a 20-30 μm or 80-90 μm thick z-cut quartz sample (see Fig. 1a). The quartz sample was the reference standard for the impedance matching measurement. The glue layer was kept below 2 μm thick. The other side of the quartz, illuminated by the laser drive, had a 20 μm CH ablator to reduce hard x-ray generation. The free surface of the diamond had an anti-reflective coating to minimize back-reflections. The diamond and quartz densities were $3.51\ \text{g}/\text{cm}^3$ and $2.65\ \text{g}/\text{cm}^3$ respectively. At the probe laser wavelength of 532 nm, the index of refraction of the diamond and quartz samples were 2.42 and 1.55 respectively.

Shock velocities in the quartz and diamond samples were measured using a line-imaging Velocity Interferometer System for Any Reflector (VISAR)^{23–26} which measures the Doppler shift of a moving reflector. By design, drive pressures were kept sufficiently high in these experiments that the shock front was optically reflecting in quartz²⁷ and diamond,¹⁷ allowing the VISAR to provide a direct, time-resolved measurement of the shock velocity in both materials. Two VISAR's were run concurrently on each shot, the first using an 18 mm etalon and the second using a 7 mm etalon.²⁸ This corresponds respectively to velocity sensitivities of 1.766 and 4.465 $\mu\text{m}/\text{ns}/\text{fringe}$ for quartz and 1.129 and 2.854 $\mu\text{m}/\text{ns}/\text{fringe}$ for diamond. Only measurements from the high sensitivity VISAR were used in the analysis; the less sensitive VISAR was used to resolve the 2π phase shift ambiguities which occur at shock break-out. Post-processing of the VISAR images using Fourier Transform methods determines the fringe position to $\sim 5\%$ of a fringe with larger errors being incurred on shots with particularly low shock reflectivities; the resulting velocities were measured to 0.3-1.1% precision since shock speeds were high enough to cause a significant number of fringe shifts. The probe source for the VISAR was an injection-seeded, Q-switched, yttrium-aluminum garnet laser, operating at a wavelength of 532 nm. Streak cameras with temporal windows of 9 and 15 ns were used to detect the reflected probe signal. The time resolution of the diagnostic was

dominated by the 90 or 40 ps delay time in each interferometer.

Twelve shots were taken at diamond pressures between 6 and 19 Mbar. Below 6 Mbar the shock front in diamond is no longer optically reflecting, making it impossible to perform the highly-precise VISAR measurements of the shock velocity. As will be shown, at pressures much above 19 Mbar in diamond (corresponding to ~ 15 Mbar in quartz), systematic uncertainties in the quartz reference standard make it difficult to perform highly-accurate measurements.

III. HIGH PRECISION VELOCITY MEASUREMENTS

A significant increase in the precision of velocity measurements was achieved in this experiment compared to previous laser-driven shock wave experiments on diamond.^{20,21} This improvement was largely accomplished by implementing quartz as an impedance matching standard, thus allowing a completely VISAR-based measurement of shock velocities and eliminating the need for transit time measurements.^{29,30} In many laser-driven shock wave experiments the limited precision of transit time measurements, at 2-3%, is the single greatest source of uncertainty and explains why the diamond Hugoniot measurements by Nagao *et al.*,²⁰ (using an Aluminum standard) and many of those by Brygoo *et al.*²¹ (using a quartz standard) have large error bars. Although a few data points from Brygoo *et al.*²¹ utilized the same all-VISAR measurement described in this experiment, those measurements were performed with a lower sensitivity interferometer and had poor quality streak records as evidenced by the example shown in Fig. 1b of Ref.²¹.

Use of the VISAR to measure velocities in a quartz standard also solved the problem posed by unsteady laser-driven shock waves. Since unsteady shocks can vary in velocity by several percent over typical transit time intervals of 1-2 ns this is a large, and potentially difficult to quantify, source of error. Using the time-resolved VISAR measurement allowed velocities to be tracked during transit through the samples; values immediately before and after the shock crossed the quartz-diamond interface were then used in the impedance matching analysis (see below).

It is important to recognize that the presence of a non-steady wave, while it can severely compromise a transit time measurement, does not compromise the validity of the impedance matching method itself. The impedance matching construct relies on the condition that the pressure and particle velocity is continuous across the common interface between two materials; these materials undergo shock, re-shock, or release in order to maintain this condition. Such behavior follows immediately from mass and momentum continuity across a surface and is true whether or not the flow is steady. The complication for unsteady waves is one of measurement accuracy: mea-

sured shock velocities must be determined immediately before and after the shock transits the interface if they are to be associated with the impedance matched states.

The sample VISAR trace shown in Fig. 1b and the accompanying velocity lineout in Fig. 1c illustrates how the shock velocity is tracked continuously through the quartz and diamond samples. Even with this highly time-resolved velocity measurement however, small corrections are still required to accurately determine the shock velocity at the instant the shock wave crosses the interface. This is because, as seen in Fig. 1c, when the shock transits the quartz-diamond interface the velocity change is not instantaneous. A short transition interval of ~ 300 ps is caused by (i) the finite time resolution of the VISAR, and (ii) the presence of a ~ 1 - 2 μm glue layer at the interface which causes a rapid rattle up of the shock velocity. To account for this, velocities at the ‘instant’ (t_{imp}) the shock crosses the interface are determined by linearly fitting velocities in a brief interval just before and after this blurred transition period (shown as Δ_1 and Δ_2 in Fig. 1c) and extrapolating the fits to t_{imp} positioned at the center of the transition (given by the dotted line in Fig. 1c). Errors in these extrapolations are included in the uncertainty analysis. This type of analysis can be compromised if there is a sudden increase in the drive pressure which results in a change in the shock velocity at the instant when the wave crosses the interface. To avoid this problem these experiments often employed a gently decaying shock wave which attenuates smoothly in time.

It should be noted that it is not just unsteady shocks that require this type of fitting analysis. Even with a perfectly steady wave, it is best to linearly fit VISAR data over a finite time interval (instead of just taking the velocity at a single instant) in order to smooth out statistical uncertainties and increase precision.

IV. IMPEDANCE MATCHING ANALYSIS

Impedance matching^{31,32} (IM) is used to determine the diamond particle velocity (U_{pC}), pressure (P_C), and density (ρ_C) from the measured shock velocities in quartz, U_{sQ} , and diamond, U_{sC} . This requires knowledge of both the principal Hugoniot and the re-shock behavior of the quartz standard. An IM method has been constructed using the experimentally-derived principal Hugoniot for quartz and a constant Gruneisen parameter. Systematic errors based on uncertainties in the quartz Hugoniot and re-shock are propagated throughout. Use of this technique for impedance match measurements in release was described by Brygoo *et al.*³³

The quartz principal Hugoniot was measured previously²⁹ and found to have linear U_s - U_p behavior given by $U_s = a_0 + a_1(U_p - \beta)$ where $a_0 = 20.57 \pm 0.15$, $a_1 = 1.291 \pm 0.036$ and $\beta = 12.74$. Errors include both measurement uncertainties as well as systematic uncertainties in the Aluminum EOS used in the analysis

of the quartz data.³⁴

The quartz re-shock Hugoniot is quite well approximated by a reflection of the principal Hugoniot in the P - U_p plane since the increase in shock pressure upon transit from the quartz into the diamond is only 20-30%. Small deviations from this reflected Hugoniot behavior are estimated using the Gruneisen parameter, Γ , which determines the pressure difference between equal-volume states on the double and single shock Hugoniots. Using the shock Hugoniot relations and the thermodynamic definition of the Gruneisen parameter the pressure on the quartz second shock Hugoniot, $P_{H2}(v)$, at a given volume, v , is given by

$$P_{H2}(v) = P_{H1}(v) + (2v/\Gamma + v - v_1)^{-1} \times [(P_{H1}(v_1) - P_0)(v_0 - v) + (P_{H1}(v) - P_0)(v_1 - v_0)] \quad (1)$$

where $P_{H1}(v)$ is the corresponding pressure on the single-shock Hugoniot at volume v . The second shock originates from a first shock state of volume v_1 and pressure $P_{H1}(v_1)$, with P_0 and v_0 being the un-shocked pressure and volume respectively. Further use of the Hugoniot relations shows that the particle velocity on the second shock Hugoniot, $U_{H2}(v)$, is given by

$$U_{H2}(v) = U_{H1}(v_1) \pm \sqrt{(P_{H2}(v) - P_{H1}(v_1))(v_1 - v)} \quad (2)$$

where $U_{H1}(v_1)$ is the particle velocity of the single-shock state from which the second shock originates. In this experiment, the sign of the square root is always negative since the shock wave is reflected (rather than catching up).

Impedance matching requires that the quartz re-shock pressure and velocity given by Eqs. 1 and 2 are related directly to the measured diamond shock velocity, U_{sC} , via the Hugoniot expression:

$$P_{H2}(v) = P_0 + \rho_{0C} U_{sC} U_{H2}(v) \quad (3)$$

where ρ_{0C} is the initial density of diamond. Since the quartz shock speed is measured, and thus $P_{H1}(v_1)$ and v_1 are known, these equations can be solved for the single unknown v and then used to determine the pressure, particle velocity, and density of diamond.

The value of the Gruneisen parameter in strongly-shocked quartz was derived from solid and porous Hugoniot experiments on silica^{29,35,36} and found to be essentially constant (at $\Gamma = 0.6 \pm 0.1$) once the shock enters the high pressure fluid phase.³⁷ Examining a range of EOS models for silica over the pressure range 4-17 Mbar applicable to this experiment, it was found that $\Gamma = 0.64 \pm 0.11$, in good agreement with experiment. The model-derived value and uncertainty is used in the analysis and is the only model-based parameter used in the impedance matching calculations.

Systematic uncertainties in the impedance matching analysis arise from uncertainties in 3 coefficients: a_0 and a_1 from the quartz principal Hugoniot, and the

Gruneisen parameter, Γ . These uncertainties are propagated throughout the analysis and combined in quadrature with the random uncertainties (arising from velocity measurements) to determine the total error. The relative importance of the various error contributions changes with shock pressure and will be described in the next section.

V. RESULTS

The results are listed in Table I and shown in both the U_s - U_p plane (Fig. 2) and the P - ρ plane (Fig. 3). The total uncertainty for these data is given by black error bars, corresponding to a quadrature sum of both random and systematic uncertainties; overlapping them, and always smaller, are a set of red error bars which correspond only to the random uncertainties. These data indicate an approximately linear U_s - U_p Hugoniot which for reference is given (in units of km/s) by $U_s = (24.31 \pm 0.02) + (1.009 \pm 0.010)(U_p - 12.32)$. However, slight deviations from linear behavior are apparent and it is these deviations which are of interest in the discussion of melting in the next section. Such subtle effects hinge on a proper assessment of the random and systematic errors in the data.

The total uncertainty in density, shown in Fig. 4, lies between 1.2 and 2.6% and is significantly smaller than the errors in previous laser-driven shock Hugoniot measurements. Total uncertainties in ρ_C (as well as P_C and U_C) were determined by the quadrature sum of 5 different sources of error: ΔU_{sQ} , ΔU_{sC} , Δa_0 , Δa_1 , and $\Delta \Gamma$. The first two are measurement errors while the last three are systematic errors in the quartz EOS. Examining these individual error contributions (see Fig. 4) it is apparent that below 10 Mbar the dominant uncertainty is from velocity measurement errors. At low velocities the VISAR is less precise since the constant error of 5% of a fringe is a larger fraction of the total velocity; also, below 10 Mbar, the reflectivity of the diamond shock front drops rapidly,¹⁷ making the measurement of U_{sC} less accurate. At higher pressures, the density errors due to velocity measurements begin to rise again slightly since the increased compression of diamond amplifies errors in the measured velocity; thus, despite the decrease in the velocity uncertainty itself, errors in density begin to increase again. Above 10 Mbar, systematic errors dominate. These arise primarily from uncertainties in the slope of the quartz Hugoniot and the Gruneisen parameter. Precisely measuring the diamond Hugoniot above 20 Mbar will require improving the accuracy of the quartz standard.

The effects of preheat, shock curvature, and shock unsteadiness were considered but were found to be undetectable. Systematic shifts due to x-ray preheat were explored in the regime of 10 Mbar by examining data taken using either thin ($\sim 20 \mu\text{m}$) or thick ($\sim 90 \mu\text{m}$) quartz pushers. The latter provides >100 times the x-

ray attenuation for x-rays <4 keV. As shown in Table I, shots 48882 (thin pusher) and 49615 (thick pusher) both at pressures of ~ 10 Mbar have almost identical inferred densities. This indicates that, at least in this pressure regime and below, the effects of pre-heat on the measured compression are negligible.

Shock curvature can be a significant source of error for transit time based measurements across a step since break-out times are measured at spatially-separated locations on the target; however, this is not a problem here since velocity measurements in both quartz and diamond were performed at the same point in space. Shock curvature could also cause the VISAR to measure a velocity component which is less than the speed of the shock front. Based on the slightly curved break-out times across the target (shown in Fig. 1b) the largest incidence angles were ~ 2 degrees from normal. This would cause an error in the measured velocity of $\ll 0.1\%$.

Shock unsteadiness effects were investigated by checking for any differences between Hugoniot points taken at similar pressures but with varying degrees of shock steadiness. The measured acceleration of shock velocities in quartz and diamond at the impedance matching instant are listed in curly brackets in Table I. From these data it can be seen that, for example, the quartz shock velocity acceleration on shot #59565 (-2.72 km/s/ns) is nearly three times that on shot #49616 (-1.02 km/s/ns) yet the Hugoniot points are almost identical. This is consistent with the argument presented in Section III that shock unsteadiness effects are not important in impedance matching experiments as long as the velocities are taken at the instant the shock transits the interface between the two materials.

VI. DISCUSSION

These new high precision measurements of the diamond Hugoniot directly overlap the pressure range explored in recent laser-driven shock experiments by Nagao *et al.*²⁰ and Brygoo *et al.*²¹ The data from Nagao *et al.*,²⁰ despite their large uncertainties (see Section III), are in general agreement with our measurements. For proper comparison, we have re-analyzed those data using an Aluminum EOS which is in better agreement with available absolute Al Hugoniot data,³⁴ resulting in a slightly softer diamond Hugoniot than that reported originally by Nagao *et al.*²⁰ Data from experiments by Brygoo *et al.*,²¹ show a $\sim 14\%$ density jump at ~ 7.5 Mbar which was claimed as evidence for melting at a negative Clapeyron slope. Our measurements between 6 and 10 Mbar show no indication of such a large volume collapse.

Comparing our data with the lower pressure measurements from Pavlovskii¹⁸ does suggest the presence of a $\sim 3\%$ density increase at 6 Mbar, as shown in Fig. 3. This discontinuity may be a signature of entry into the diamond-liquid coexistence regime as described below, although it could instead be an artefact of unknown ex-

perimental uncertainties (Pavlovskii did not report errors). It is not possible to collect diamond Hugoniot data below 6 Mbar using the high precision technique discussed in this paper since the diamond shock front is no longer sufficiently optically reflecting for the VISAR measurement.¹⁷

Hugoniot calculations based on the multi-phase free-energy model of Fried and Howard,¹¹ which showed a dramatic softening of the Hugoniot in the solid-liquid coexistence region, disagree with our measurements. It appears that the compressibility of the fluid in that model was too high, resulting in a large negative slope in the melting curve and thus an overly large density jump along the Hugoniot. A free energy model from the Sesame³⁸ database, which does not include multiple phases, disagrees slightly with our measurements between 6 and 10 Mbar but is in quite good agreement at higher pressures.

Ab initio predictions by Correa *et al.*^{9,15} indicate that the Hugoniot lies in the diamond phase below 6 Mbar and the pure liquid phase above ~ 10 Mbar, with an implied solid-liquid coexistence regime in between. Romero and Mattson¹⁶ predicted a similar Hugoniot although their melt region was not independently calculated. These Hugoniot calculations are shown in Figs. 2 and 3, with the gap in each line representing the coexistence region. Pavlovskii's data is in good agreement with the predicted solid Hugoniot, while our measurements are in agreement with the predicted liquid Hugoniot, at least up to the maximum calculated pressures of ~ 13 Mbar. This shows that the Hugoniots for the pure diamond and pure liquid phases almost fall along the same linear U_s - U_p relation.

Our measurements suggest that the solid-liquid coexistence regime has a slightly higher density (by 2-3%) than would be expected from a simple interpolation between pure solid and liquid states. This mixed phase region between 6 and 10 Mbar is not calculated explicitly by the *ab initio* theories. Instead, the additional postulate of volume-weighted linear mixing, which assumes a homogeneous mixture with negligible interfacial free energy, is commonly used to treat such a mixed region.¹⁵ Additional complexity arises in the case of shock melting of diamond because the Hugoniot is predicted to pass through a BC8-liquid coexistence phase just before completion of melting, between about 9 and 10 Mbar.¹⁵ More sophisticated calculations, beyond the linear mixing approximation, will be required to better understand how such mixed phases behave at high pressure.

VII. CONCLUSIONS

Precision measurements of the diamond Hugoniot between 6 and 19 Mbar have been used to probe an ex-

tensive region of the high pressure carbon phase diagram, including the dense, high-temperature fluid and the diamond-liquid coexistence regime. These data, which represent a significant improvement over earlier laser-driven shock wave measurements on diamond, are in general agreement with recent *ab initio* model calculations of the diamond Hugoniot in the pure liquid phase from 10 to 13 Mbar. The extraordinarily large extent of the diamond-BC8-liquid coexistence regime between 6 and 10 Mbar may be a valuable way to test theories of how mixed phases behave at ultra-high pressure.

Acknowledgments

We thank the Omega operations crew for help in carrying out the experiments, Mark Bonino and the Omega target fabrication group for their outstanding work, and Walter Unites for his assistance throughout. This work was performed under the auspices of the U.S. Department of Energy by Lawrence Livermore National Laboratory in part under Contract W-7405-Eng-48 and in part under Contract DE-AC52-07NA27344, and by the University of Rochester under Cooperative Agreement No. DE-FC03-92SF19460.

VIII. APPENDIX

Prior to the experiments reported above, we performed several measurements of the diamond Hugoniot using an Aluminum or Molybdenum standard.³⁹ Shock velocities in the standard were determined using transit time measurements (since both Al and Mo are optically opaque) while shock velocities in the diamond were determined using the VISAR. In order to account for shock unsteadiness, the time-resolved measurements of the velocity history in diamond were used to infer the velocity history in the opaque standard. However, the limited precision of the transit time measurement (as discussed in Section III) resulted in data with much larger error bars than those in the improved experiment described above.

A comparison of the two data sets shows that, despite the large random uncertainties, the fit to the less precise data is in quite good agreement with the new measurements (see Fig. 5 and 6). The best linear U_s - U_p fit to the data is given (in units of km/s) by $U_s = (25.73 \pm 0.30) + (1.054 \pm 0.090)(U_p - 14.010)$ and is labeled on the plots as 'Bradley fit'. Since these older data include the highest diamond Hugoniot measurements ever performed (up to 36 Mbar), we include them here for reference (see Table II).

* Author to whom correspondence should be addressed: hicks13@llnl.gov

¹ D. R. Lide, ed., *CRC Handbook of Chemistry and Physics*

- (CRC Press/Taylor and Francis, Boca Raton, FL, Internet Version 2008), 88th ed.
- ² F. P. Bundy, W. A. Bassett, M. S. Weathers, R. J. Hemley, H. K. Mao, and A. F. Goncharov, *Carbon* **34**, 141 (1996).
 - ³ M. T. Yin and M. L. Cohen, *Phys. Rev. Lett.* **50**, 2006 (1983).
 - ⁴ F. P. Bundy, *The Journal of Chemical Physics* **38**, 631 (1963).
 - ⁵ J. W. Shaner, J. M. Brown, C. A. Swenson, and R. G. McQueen, *J. Phys. (Paris) Colloqu.* **45**, c8 (1984).
 - ⁶ D. A. Young and R. Grover, in *Shock Compression of Condensed Matter - 1987*, edited by S. Schmidt and N. C. Holmes (North Holland, Amsterdam, 1988), pp. 131–4.
 - ⁷ M. van Thiel and F. H. Ree, *Intl. J. ThermoPhys.* **10**, 227 (1989).
 - ⁸ A. M. Molodets, M. A. Molodets, and S. S. Nabatov, in *Shock Compression of Condensed Matter - 1997*, edited by S. Schmidt, Dandekar, and G. Forbes (AIP, 1998), p. 91.
 - ⁹ A. A. Correa, S. A. Bonev, and G. Galli, *Proc. Nat. Acad. Sciences* **103**, 1204 (2006).
 - ¹⁰ X. Wang, S. Scandolo, and R. Car, *Phys. Rev. Lett.* **95**, 185701 (2005).
 - ¹¹ L. E. Fried and W. M. Howard, *Physical Review B (Condensed Matter and Materials Physics)* **61**, 8734 (2000).
 - ¹² M. P. Grumbach and R. M. Martin, *Phys. Rev. B* **54**, 15730 (1996).
 - ¹³ S. Fahy and S. G. Louie, *Phys. Rev. B* **36**, 3373 (1987).
 - ¹⁴ W. J. Nellis, A. C. Mitchell, and A. K. McMahan, *J. Appl. Phys.* **90**, 696 (2001).
 - ¹⁵ A. A. Correa, L. X. Benedict, D. A. Young, E. Schwegler, and S. A. Bonev, *Physical Review B (Condensed Matter and Materials Physics)* **78**, 024101 (pages 13) (2008).
 - ¹⁶ N. A. Romero and W. D. Mattson, *Physical Review B (Condensed Matter and Materials Physics)* **76**, 214113 (pages 8) (2007).
 - ¹⁷ D. K. Bradley, J. H. Eggert, D. G. Hicks, P. M. Celliers, S. J. Moon, R. C. Cauble, and G. W. Collins, *Phys. Rev. Lett.* **93**, 195506 (2004).
 - ¹⁸ M. N. Pavlovskii, *Sov. Phys. Solid State* **13**, 741 (1971).
 - ¹⁹ K. Kondo and T. J. Ahrens, *Geophys. Res. Lett.* **10**, 281 (1983).
 - ²⁰ H. Nagao, K. G. Nakamura, K. Kondo, N. Ozaki, K. Takamatsu, T. Ono, T. Shiota, D. Ichinose, K. A. Tanaka, K. Wakabayashi, et al., *Phys. Plasmas* **13**, 052705 (2006).
 - ²¹ S. Brygoo, E. Henry, P. Loubeyre, J. Eggert, M. Koenig, B. Loubias, A. Benuzzi-Mounaix, and M. Rabec Le Gloahhec, *Nat. Mater.* **6** (2007).
 - ²² T. R. Boehly, D. L. Brown, R. S. Craxton, R. L. Keck, J. P. Knauer, J. H. Kelly, T. J. Kessler, S. A. Kumpan, S. J. Loucks, S. A. Letzring, et al., *Opt. Comm.* **133**, 495 (1997).
 - ²³ L. M. Barker and R. E. Hollenbach, *J. Appl. Phys.* **43**, 4669 (1972).
 - ²⁴ L. M. Barker and K. W. Schuler, *J. Appl. Phys.* **45**, 3692 (1974).
 - ²⁵ P. M. Celliers, G. W. Collins, L. B. D. Silva, D. M. Gold, and R. Cauble, *Appl. Phys. Lett.* **73**, 1320 (1998).
 - ²⁶ P. M. Celliers, D. K. Bradley, G. W. Collins, D. G. Hicks, T. R. Boehly, and W. J. Armstrong, *Rev. Sci. Instr.* **75**, 4916 (2004).
 - ²⁷ D. G. Hicks, T. R. Boehly, J. H. Eggert, J. E. Miller, P. M. Celliers, and G. W. Collins, *Phys. Rev. Lett.* **97**, 025502 (2006).
 - ²⁸ On a single shot (#48880) the 18 mm etalon was replaced by a 45 mm etalon.
 - ²⁹ D. G. Hicks, T. R. Boehly, P. M. Celliers, J. H. Eggert, E. Vianello, D. D. Meyerhofer, and G. W. Collins, *Phys. Plasmas* **12**, 082702 (2005).
 - ³⁰ T. R. Boehly, D. G. Hicks, P. M. Celliers, T. J. B. Collins, R. Earley, J. H. Eggert, D. Jacobs-Perkins, S. J. Moon, E. Vianello, D. D. Meyerhofer, et al., *Phys. Plasmas* **11**, L49 (2004).
 - ³¹ J. M. Walsh, M. H. Rice, R. G. McQueen, and F. L. Yarger, *Phys. Rev.* **108**, 196 (1957).
 - ³² Y. B. Zeldovich and Y. P. Raizer, *Physics of Shock Waves and High Temperature Hydrodynamic Phenomena* (Dover Publications Inc., Minolta, N.Y., 2002).
 - ³³ S. Brygoo, submitted for publication.
 - ³⁴ P. M. Celliers, G. W. Collins, D. G. Hicks, and J. H. Eggert, *J. Appl. Phys.* **98**, 113529 (2005).
 - ³⁵ R. F. Trunin, *Phys. Usp.* **37**, 1123 (1994).
 - ³⁶ R. F. Trunin, *Shock Compression of Condensed Materials* (Cambridge University Press, Cambridge, 1998).
 - ³⁷ Silica is a particularly valuable impedance matching standard because of the ready availability of polymorphs with different initial densities. This allows an accurate determination of the Gruneisen parameter up to very high pressures.
 - ³⁸ S. P. Lyon and J. Johnson, *Tech. Rep. LA-CP-98-100*, Los Alamos National Laboratory (1998).
 - ³⁹ D. K. Bradley, P. M. Celliers, J. H. Eggert, D. G. Hicks, D. H. Munro, and G. W. Collins (2005), unpublished.

TABLE I: Diamond-phase carbon Hugoniot results from impedance matching to a quartz standard. U_{sQ} and U_{sC} are the measured shock velocities in quartz and diamond with random (i.e. measurement) errors; values in curly brackets are the instantaneous acceleration of the shock velocity in km/s/ns at the impedance matching instant. $P_C(\text{ran,sys})$, $\rho_C(\text{ran,sys})$, and $U_C(\text{ran,sys})$ are the pressure, density, and particle velocity of shocked diamond inferred from impedance matching calculations showing both random and systematic errors. Random errors come from measurement uncertainties in U_{sQ} and U_{sC} and systematic errors come from uncertainties in the principal and re-shock Hugoniots of quartz. Shot numbers with an asterisk indicate targets with a thin quartz pusher; others had a thick quartz pusher.

Expt.	U_{sQ} km/s	U_{sC} km/s	$P_C(\text{ran,sys})$ Mbar	$\rho_C(\text{ran,sys})$ g/cm ³	$U_C(\text{ran,sys})$ km/s
49976	17.29±0.12 {-0.83}	20.39±0.24 {0.45}	6.25±(0.09,0.05)	6.14±(0.09,0.04)	8.73±(0.11,0.07)
50364	18.83±0.18 {-1.53}	21.66±0.13 {-1.18}	7.51±(0.12,0.07)	6.45±(0.10,0.05)	9.87±(0.16,0.09)
49974	19.37±0.10 {-0.99}	22.05±0.11 {-0.05}	7.96±(0.07,0.08)	6.58±(0.06,0.05)	10.28±(0.09,0.10)
49614	19.96±0.10 {-0.38}	22.46±0.08 {-1.05}	8.46±(0.07,0.08)	6.72±(0.06,0.06)	10.73±(0.09,0.11)
51565	20.88±0.12 {-2.72}	23.36±0.07 {-0.87}	9.34±(0.09,0.10)	6.85±(0.07,0.07)	11.40±(0.10,0.12)
49616	20.94±0.12 {-1.02}	23.46±0.07 {-0.93}	9.41±(0.09,0.10)	6.85±(0.07,0.07)	11.43±(0.10,0.12)
49615	21.11±0.11 {-1.36}	23.72±0.07 {-1.02}	9.60±(0.08,0.11)	6.83±(0.06,0.07)	11.54±(0.09,0.13)
48882*	21.89±0.11 {-4.25}	24.22±0.07 {-1.45}	10.32±(0.09,0.12)	7.03±(0.06,0.08)	12.14±(0.10,0.14)
48448*	22.59±0.12 {-3.83}	25.02±0.09 {-1.84}	11.08±(0.10,0.13)	7.08±(0.07,0.09)	12.62±(0.11,0.15)
48880*	24.88±0.06 {-2.32}	26.33±0.07 {0.71}	13.34±(0.05,0.17)	7.77±(0.05,0.12)	14.43±(0.05,0.18)
49450*	27.63±0.11 {-3.79}	28.42±0.08 {-3.31}	16.49±(0.11,0.23)	8.39±(0.08,0.16)	16.53±(0.10,0.23)
49447*	29.74±0.15 {-2.91}	30.19±0.09 {-1.98}	19.18±(0.15,0.30)	8.77±(0.11,0.20)	18.10±(0.14,0.28)

TABLE II: (Appendix) Previously unpublished impedance-match Hugoniot data for diamond-phase carbon obtained using an Aluminum or Molybdenum standard. Subscript R refers to parameters of the reference standard, and C of the sample. Columns indicate the initial densities $\rho_{0R,C}$, measured shock speed in the reference standard U_{sR} and non-steadiness correction ΔU_{sR} , measured shock speed in the sample U_{sC} , and the inferred particle speed u_{pC} , pressure P_C and density ρ_C in the diamond samples. Random and systematic uncertainties are separately listed for each quantity.

Expt.	ρ_{0R} g cm ⁻³	ρ_{0C} g cm ⁻³	U_{sR} km/s	ΔU_{sR} km/s	U_{sC} km/s	$u_{pC}(\text{ran, sys})$ km/s	$P_C(\text{ran, sys})$ GPa	$\rho_C(\text{ran, sys})$ g cm ⁻³
20547(Al)	2.70	3.51	22.08±0.75	0.00	23.12±0.34	11.88±(0.74, 0.09)	964±(60, 8)	7.22±(0.50, 0.06)
24278(Al)	2.70	3.51	22.28±0.60	-1.28	24.58±0.26	11.79±(0.58, 0.09)	1017±(51, 8)	6.75±(0.32, 0.05)
24365(Al)	2.70	3.51	23.59±0.39	-0.16	23.82±0.26	13.24±(0.39, 0.11)	1107±(33, 10)	7.90±(0.33, 0.08)
24294(Al)	2.70	3.51	24.36±0.68	-0.12	26.18±0.26	13.51±(0.67, 0.12)	1242±(62, 11)	7.25±(0.40, 0.07)
24288(Al)	2.70	3.51	29.92±0.91	2.31	30.70±0.27	18.11±(0.92, 0.22)	1952±(100, 23)	8.56±(0.65, 0.15)
20541(Al)	2.70	3.51	36.74±1.76	0.83	34.95±0.35	24.12±(1.82, 0.34)	2960±(220, 40)	11.3±(1.9, 0.4)
26397(Mo)	10.2	3.51	30.96±0.92	0.58	39.08±0.33	26.10±(1.11, 0.88)	3580±(150, 120)	10.57±(0.92, 0.72)

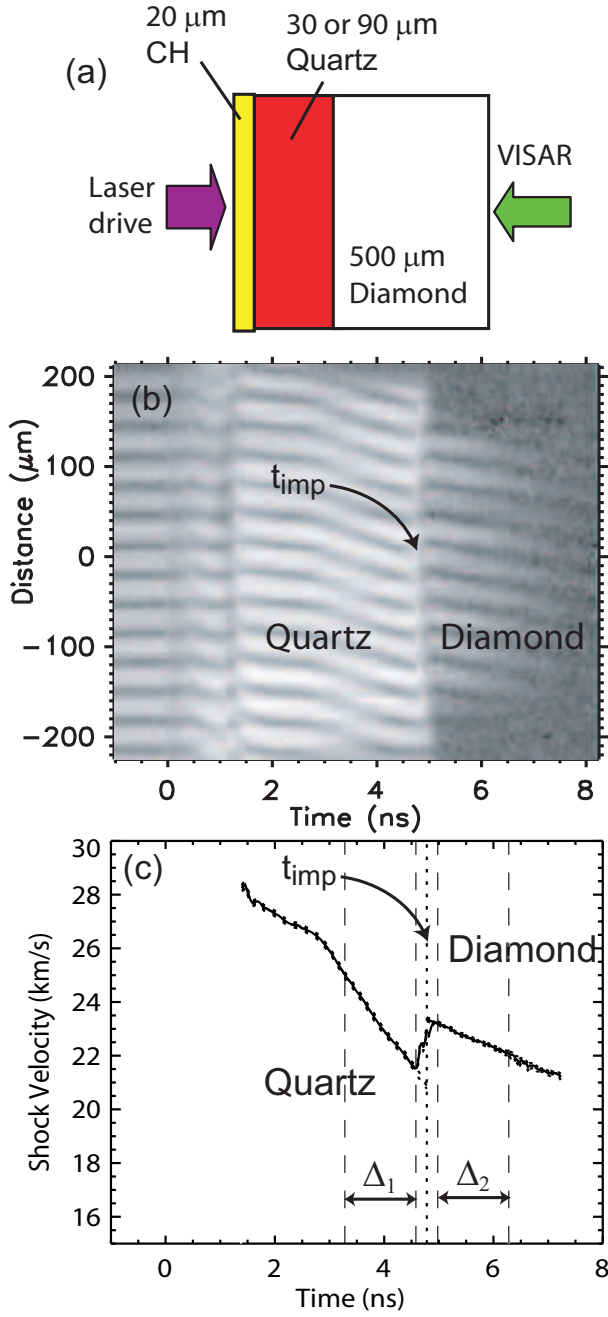


FIG. 1: (a) Schematic of the quartz-diamond impedance matching targets. (b) Line VISAR trace showing reflecting shock fringes in quartz and diamond. The time that the shock crosses the interface between the two materials is labeled as t_{imp} . (c) Velocity history extracted from the VISAR trace in (b); dotted lines above and below the lineout indicate measurement errors; t_{imp} is the instant at which the impedance matching velocities are taken. To precisely determine the velocity at t_{imp} , a linear fit is taken of the velocities over a neighboring time interval Δ_1 (or Δ_2) and extrapolated forward (or backward) to t_{imp} .

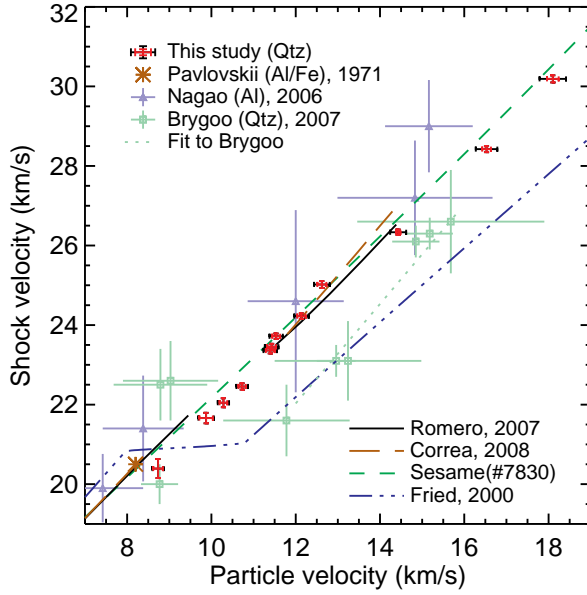


FIG. 2: Shock velocity versus particle velocity plot of the diamond Hugoniot in and above the expected^{15,17} melt region (corresponding to $20 \lesssim U_s \lesssim 24$ km/s). For data from this study, random errors are given by red error bars while the total uncertainties, including systematic uncertainties from the quartz EOS, are given by black error bars. These data are in general agreement with *ab initio* calculations from Romero and Mattson¹⁶ and Correa *et al.*¹⁵ but disagree with previous measurements by Brygoo *et al.*²¹ or with the free energy model of Fried and Howard.¹¹

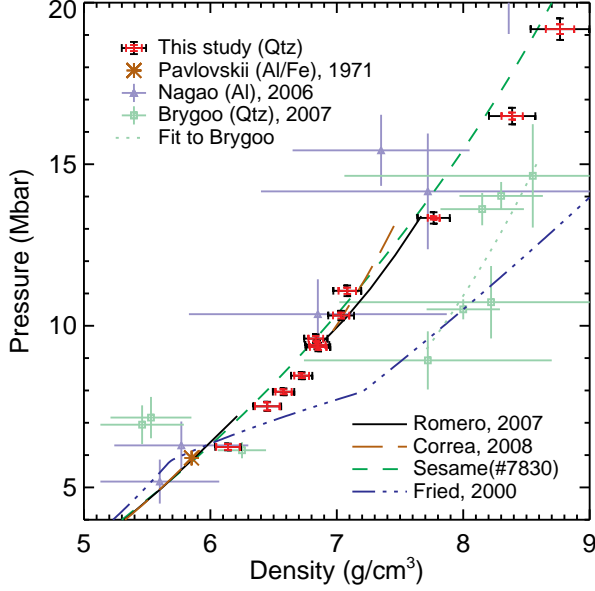


FIG. 3: Pressure versus density plot of the diamond Hugoniot in and above the expected^{15,17} melt region (corresponding to $6 \lesssim P \lesssim 10$ Mbar). For data from this study, random errors are given by red error bars while the total uncertainties, including systematic uncertainties from the quartz EOS, are given by black error bars.

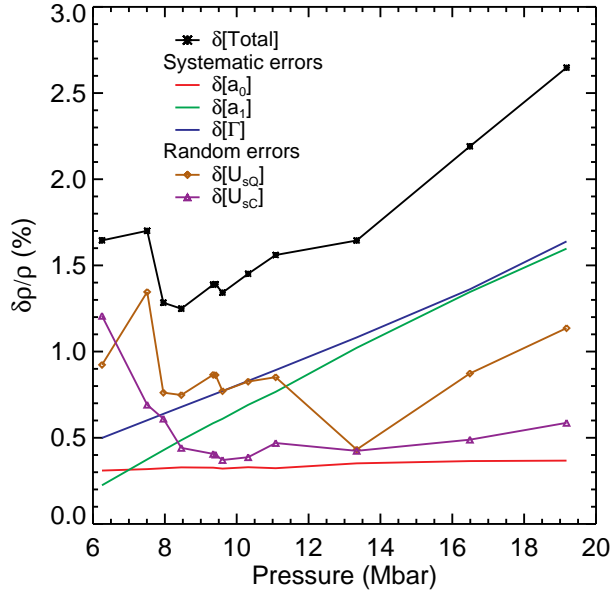


FIG. 4: The total uncertainty in density is determined by a quadrature sum of 3 systematic components and 2 random components. Systematic errors arise from uncertainties in the quartz EOS as given by Hugoniot fit parameters (a_0 and a_1) and the Gruneisen parameter (Γ). Random errors arise from uncertainties in the shock velocities in quartz (δU_{sQ}) and diamond (δU_{sC}). Below ~ 10 Mbar, random errors dominate.

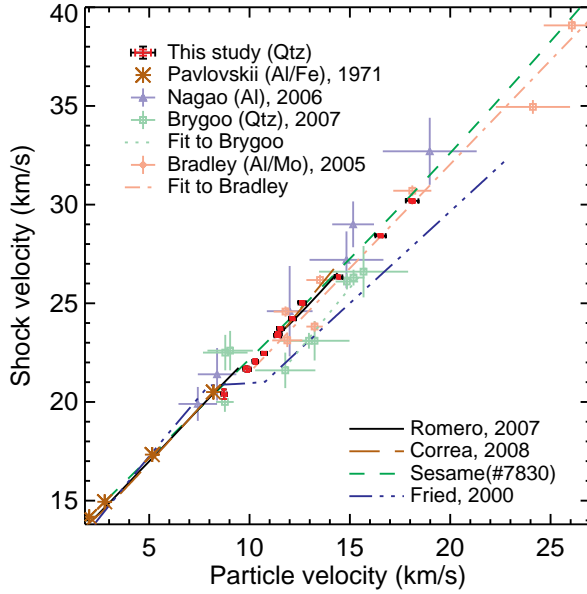


FIG. 5: The diamond Hugoniot shown in Fig. 2 expanded to include unpublished measurements from Bradley *et al.*³⁹ up to 36 Mbar. These data suggest that above 20 Mbar the Hugoniot still approximately follows the linear U_s - U_p fit found at lower pressures.

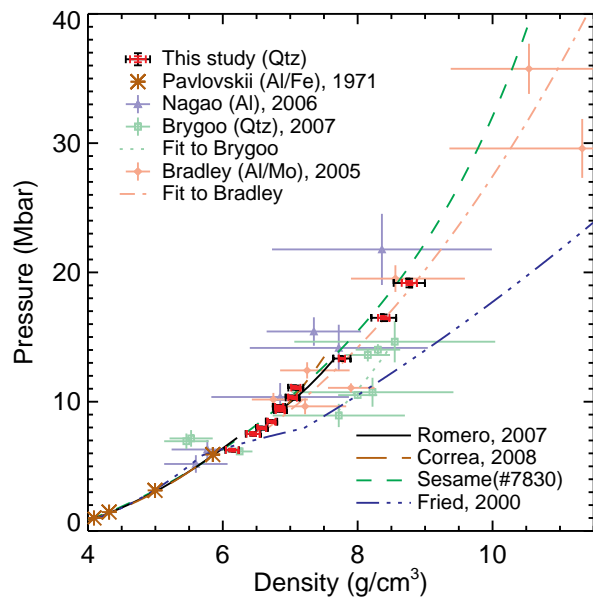


FIG. 6: A view of the diamond Hugoniot measurements shown in Fig. 3 expanded to include unpublished measurements from Bradley *et al.*³⁹ up to 36 Mbar.